COMPACTION WAVES IN GRANULAR HMX

Ralph Menikoff and Edward Kober

Theoretical Division, Los Alamos National Laboratory, Los Alamos, NM 87544

Abstract. Piston driven compaction waves in a granular bed are simulated with a two-dimensional continuum mechanics code in which individual grains are resolved. The constitutive properties of the grains are modeled with a hydrostatic pressure and a simple elastic-plastic model for the shear stress. Parameters are chosen to correspond to inert HMX, and the initial bed chosen to represent a tightly packed random grain distribution with 19% porosity. By varying the piston velocity, waves were obtained ranging from weak partly compacted waves to strong fully compacted waves. The average stress and wave speed are compatible with the porous Hugoniot locus for uniaxial strain. However, the heterogeneities give rise to stress concentrations which lead to localized plastic flow. For weak waves, plastic deformation is the dominant dissipative mechanism and leads to dispersed waves that spread out in time. In addition to dispersion, the granular heterogeneities give rise to subgrain spatial variation in the thermodynamic variables. The peaks in the temperature fluctuations, known as hot-spots, are in the range that would have a critical effect on ignition sensitivity.

INTRODUCTION

At high pressures a granular material behaves much like a fluid. Qualitatively, the wave behavior of a granular material is determined by the Euler equations supplemented with a degree of freedom for porosity and an equation of state such as given by the P–α model (4, 3). Porosity lowers the sound speed and leads to compaction waves in which the compression following the wave front results mostly from the decrease in porosity. Compared to a shock wave, a larger volume change occurs across a compaction wave. The resulting $P\Delta V$ Hugoniot energy leads to a higher bulk temperature.

One important application of a granular material is as a model for a damaged explosive. Damage is known to increase the sensitivity of an explosive to initiation. For weak stimuli, the increased bulk temperature of a compaction wave is still well below the ignition temperature. The enhanced sensitivity is due to peaks in the temperature fluctuations, known as hot spots, and the extreme temperature dependence of an Arrhenius reaction rate. The fluctuations result from the heterogeneous nature of a granular bed. The underlying physics which gives rise to the fluctuations is not contained in a simple fluid model.

In order to understand the structure of a piston driven compaction wave in a granular material we have performed "micro-mechanical" simulations. These are computations with a continuum mechanics code over a meso-scale region on which heterogeneities and hot spots are expected to be statistically significant. Our computations were done using the COMADREJA code. This is a two-dimensional Eulerian code developed by David Benson at the University of California, San Diego. A similar code called RAVEN has been used previously to study sintering or dynamic compaction of powdered metals (1, 2). The 2-D calculations we present assume planar strain.

The form of dissipation has an important affect on the structure of a compaction wave. The code contains three dissipative mechanism; plastic work, shear viscosity and artificial bulk viscosity. The shear viscosity mocks-up the effect of frictional work at grain interfaces. The granular bed is choosen to consist of grains with material properties of HMX. Grains with a mean diameter of coarse HMX are randomly arranged but choosen to be mostly in contact.

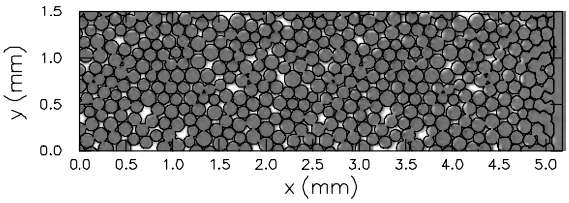

FIGURE 1. Granular bed with 19% porosity.

This corresponds to a tightly packed bed and has a porosity of about 20%. The piston velocity is varied from 200 m/s to 1000 m/s. This is well below the bulk sound speed of HMX, 2650 m/s. The waves generated are nominally planar and range from weak partly compacted waves to strong fully compacted waves.

We find that the mechanical wave properties, average pressure and wave velocity, closely correspond to the values on the porous Hugoniot locus for uniaxial strain. Stress concentrations at the contact between grains lead to plastic deformation and is responsible for the decrease in porosity behind the wave. For weak waves, plastic work is the dominant dissipative mechanism and leads to dispersed waves that spread out in time. Because of the stress concentrations, the plastic deformation is localized and leads to spatial variations in the thermodynamic variables. The hot spots are in the range that would affect ignition sensitivity.

NUMERICAL SIMULATIONS

The material properties of the grains were chosen to correspond to inert HMX. The constitutive relation consisted of a hydrostatic pressure plus a simple elastic-plastic model for the shear stress. The pressure is based on a Mie-Grüneisen equation of state with the principal Hugoniot locus as a reference curve. A linear relation for shock velocity versus particle velocity is a good approximation for the Hugoniot in the region of interest. The stress deviator is based on a constant shear modulus and a perfectly plastic, rate-independent von Mises yield condition. The parameters for the constitutive relations are listed in table 1.

Table 1. Parameters for constitutive relation of HMX.

c_0	2.65	km/s	Bulk sound speed
s	2.38	—	Slope of u_s–u_p relation
Γ/V	2.09	g/cm^3	Grüneisen coefficient
ρ_0	1.9	g/cm^3	Initial density
C_V	0.001	(MJ/kg)/K	Specific heat
G	10.	GPa	Shear modulus
Y	0.37	GPa	Yield strength

The simulations started with the granular bed shown in figure 1. The bed is roughly 30 grains long and 10 grains wide. It contains a total of 432 circular grains with an average diameter of 140 μm. The grain diameter has a uniform random variation of $\pm$10%. Computations used a cell resolution of 10 μm or roughly 14 cells per grain diameter. The value of the shear viscosity is 310 Poise. At our mesh resolution this is somewhat larger than an effective artificial viscosity of the von Neumann-Richtmeyer type. Compaction waves were driven by a piston moving from right to left. The top and bottom boundaries were chosen to be periodic.

Compaction waves were simulated for three piston velocities. For these cases, the state behind the wave predicted by the porous Hugoniot are given in table 2. Profiles of the stress σ_{xx} are shown in figure 2. The 1-D profiles are volume averages over the y-direction, namely, the transverse direction to the wave propagation. The minimum and maximum profiles indicate the range of variation. The dotted lines indicate the position and stress level based on the porous Hugoniot locus. The average stress is in good agreement while the position of the wave front is slightly behind. The delay is due to the transient formation of the wave profile. Profiles of the equivalent plastic stress are shown in figure 3.

The wave driven by the 200 m/s piston is partly compacted. The porosity profile is shown in figure 4. The leading edge of the wave is the analog of an elastic precursor. The precursor velocity, 2.9 to 3.0 km/s,

Table 2. State behind compact wave based on porous Hugoniot for uniaxial-strain.

200	500	1000	m/s	Piston velocity
1100	2100	3400	m/s	Wave speed
0.98	1	1	–	Solid volume fraction
0.34	1.6	5.2	GPa	Stress
322	424	720	K	Temperature

a) $u_p = 200\,\mathrm{m/s}$ at time = $2.0\,\mu$s

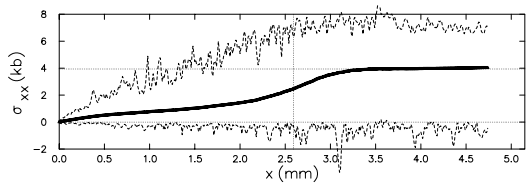

b) $u_p = 500\,\mathrm{m/s}$ at time = $1.6\,\mu$s

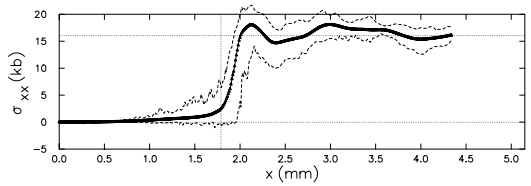

c) $u_p = 1000\,\mathrm{m/s}$ at time = $1.4\,\mu$s

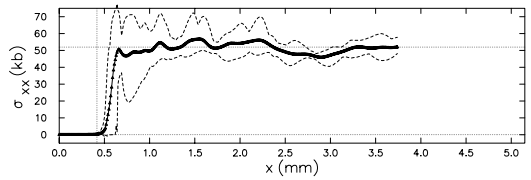

FIGURE 2. Stress profile (σ_{xx}) of compaction waves. Average, minimum and maximum are shown. Horizontal and vertical dotted lines are prediction from porous Hugoniot.

a) $u_p = 200\,\mathrm{m/s}$ at time = $1.6\,\mu$s

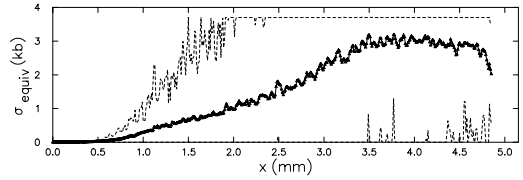

b) $u_p = 500\,\mathrm{m/s}$ at time = $1.6\,\mu$s

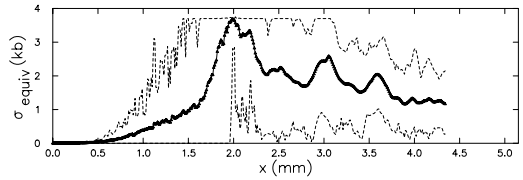

c) $u_p = 1000\,\mathrm{m/s}$ at time = $1.4\,\mu$s

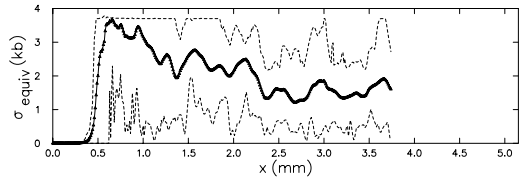

FIGURE 3. Equivalent plastic stress, $\sigma_{equiv} = \left(\frac{3}{2}\right)^{\frac{1}{2}} ||\boldsymbol{\sigma}'||$, profile of compaction waves.

is less than the longitudinal sound speed of HMX, 3.75 km/s. The lower speed is expected since a weak wave can only be transmitted between grains at their contact points. This leads to a longer effective path length and hence a lower wave speed.

The weak wave is quite dispersed. A detailed examination of the computed wave structure shows that the plastic work from compaction, $Y\varepsilon_p$, exceeds the Hugoniot energy, $\frac{1}{2}(P+P_0)\cdot(V_0-V)$. Hence, a steady wave is not possible. This is in contrast to viscous dissipation in which the wave profile can always adjust in order to obtain a steady propagating wave. For the compaction wave, the plastic strain ε_p is related to the change in the porosity. It is determined by stress concentrations due to the grain geometry and is independent of the Hugoniot relation. For stronger waves, the plastic work is less than the Hugoniot energy and other mechanism provide the additional dissipation required for a steady wave.

The stronger waves are fully compacted. The compaction begins when the maximum equivalent plastic stress reaches the yield strength. The bulk of the compaction occurs over a distance of 1 to 2 grain diameters. An elastic precursor occurs for the compaction wave driven by the 500 m/s piston. The change in plotting scale for the stress in figure 2 makes the precursor seem much weaker than for the wave driven by the 200 m/s piston. But as seen by comparing the equivalent stress in figures 3 a,b, the precursor is nearly independent of the wave strength. Because of the stress concentrations, the precursor is dispersed and not shock like as would occur for a homogeneous material. For the 1000 m/s piston the plastic wave speed exceeds the elastic wave speed

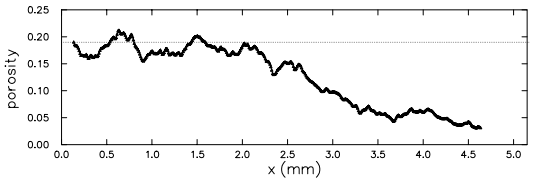

FIGURE 4. Porosity profile at $t = 2.0\,\mu$s of compaction wave driven by 200 m/s piston. Profile has been smoothed by taking running average over a length of 2 grain diameters. Dotted line is the average initial porosity.

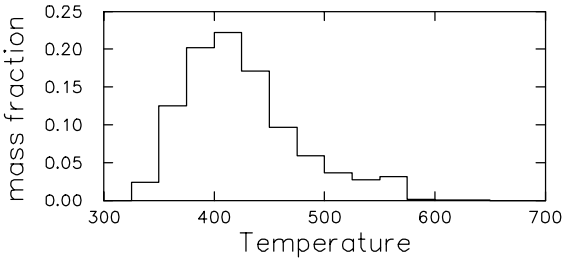

FIGURE 5. Temperature distribution behind compaction wave driven by 500 m/s piston.

and the precursor disappears. The same phenomena occurs for a homogeneous material. We also note that for the stronger waves the plastic stress decays behind the front. This is due to acoustic waves generated by the heterogeneities.

Compared to other simulations, such as those in (1, 2), we have used a longer distance of run. The difference between the elastic wave speed and the bulk compaction wave speed causes the precursor to stand out more as the run length increases. Other calculations of compaction waves in a loosely packed granular bed display a negligible precursor. This is because the acoustic coupling between grains is sufficiently weak to constrain the propagation of the precursor.

FLUCTUATIONS

The localized plastic deformation due to the stress concentrations at the contacts between grains gives rise to temperature fluctuations. The temperature distribution behind the compaction wave driven by the 500 m/s piston is shown in figure 5. The peak of the distribution is near the bulk temperature from the porous Hugoniot locus. The material at temperatures below the bulk temperature is in the interior of the grains. Hot spots correspond to the material at temperatures above the bulk temperature. The hot regions are in the vicinity of grain boundaries. The peak temperature of nearly 600 K is about the melting temperature of HMX. The burn rate becomes significant above melting. Thus, the hot spots are in the range that would have a significant effect on ignition sensitivity.

However, it should be noted that since hot spots are the fluctuations in the flow they are much more sensitive to dissipative mechanisms and numerical aspects of the computation than is the state behind the compaction wave which is largely determined by the Rankine-Hugoniot jump conditions. With our resolution, hot spots are only a few cells wide. At higher resolution we expect that the hot spots would have a smaller size but a higher peak temperature. Because of the temperature dependence of the reaction rate, this would significantly effect the average burn rate behind a weak wave. Consequently, our calculation are not yet sufficiently refined to predict ignition sensitivity. More details are available in a separate report (5).

ACKNOWLEDGMENTS

We thank Prof. David Benson, Univ. of Calif. at San Diego, for providing us with his COMADREJA code.

REFERENCES

1. Benson, D. J., *Modelling Simul. Mater. Sci. Eng.* **2**, (1994) 535–550.
2. Benson, D. J., Nesterenko, V. F., Jonsdottir, F., and Meyers, M. A., *J. Mech. Phys. Solids* **45**, (1997) 1955–1999.
3. Carroll, M., and Holt, A. C., *J. Applied Phys.* **43**, (1972) 759–761.
4. Herrmann, W., *J. Applied Phys.* **40**, (1969) 2490–2499.
5. Menikoff, R., and Kober, E., Compaction waves in granular HMX, Tech. Rep. LA-13546-MS, Los Alamos National Lab., 1999.